Osman, A. S. & Bolton, M. D. (2005). *Géotechnique* **55**, No. 6, 435–447

Simple plasticity-based prediction of the undrained settlement of shallow circular foundations on clay

A. S. OSMAN* and M. D. BOLTON*

A kinematic plastic solution has been developed for the penetration of a circular footing into an incompressible soil bed. In this solution, the pattern of deformation around the footing is idealised by a simple plastic deformation mechanism. Strain-hardening behaviour and non-linear stress–strain characteristics are incorporated. This application is different from conventional applications of plasticity theory as it can approximately predict both stresses and displacements under working conditions. This approach therefore provides a unified solution for design problems in which both serviceability and safety requirements are based directly on the stress–strain behaviour of the soil. The design strength that should limit the deformations can be selected from the actual stress–strain data recorded from a carefully specified location, and not derived using empirical safety factors. The validity of this design approach is examined against non-linear finite element analyses and field measurements of foundations on clay under short-term loading.

KEYWORDS: clays; deformation; design; footings/foundations; plasticity; theoretical analysis

Une solution plastique cinématique a été développée pour la pénétration d'une assise circulaire dans un lit de sol incompressible. Dans cette solution, la forme de la déformation autour de l'assise est idéalisée par un simple mécanisme de déformation plastique. Nous incorporons le comportement de déformation-durcissement et les caractéristiques de contrainte-déformation non linéaire. Cette application est différente des applications conventionnelles de la théorie de plasticité car elle peut approximativement prédire les contraintes et les déplacements en conditions de travail. Cette approche offre donc une solution unifiée aux problèmes de conception dans lesquels les besoins de commodité et de sécurité sont basés directement sur le comportement contrainte-déformation du sol. La force nominale qui devrait limiter les déformations peut être sélectionnée d'après la contrainte réelle – données enregistrées depuis un emplacement soigneusement spécifié et non dérivées en utilisant des facteurs de sécurité empiriques. Nous examinons la validité de cette approche de design par rapport aux analyses d'éléments finis non linéaires et aux mesures sur le terrain des fondations sur de l'argile sous charges à court terme.

INTRODUCTION

Designers have to check that shallow foundations will neither penetrate the soil subgrade in a bearing capacity failure, nor settle excessively. Bearing failure is checked using plasticity theory, whereas settlement is usually checked using elasticity. Conventionally, the calculations for settlement in saturated clay are divided into two components: immediate settlements due to deformation taking place at constant volume, and the consolidation settlement accompanying the dissipation of pore water pressure (Skempton & Bjerrum, 1957). Excessive total or differential settlements are a main cause of unsatisfactory building performance. Although this is sometimes due to unexpected consolidation, the inadequacy of linear elasticity to describe the earlier phase of undrained settlement leads to significant uncertainties. This paper proposes a resolution of the latter problem.

Circular shallow foundations are usually designed on the basis that the net imposed load under working conditions should not exceed the ultimate net imposed load that would cause collapse, divided by a safety factor. Estimation of the collapse load in the geotechnical design of circular footings is well established from plasticity theory. Several techniques based on stress characteristics, and on upper- and lower-bound theorems of limit analysis, have been used to calculate bearing capacity factors for circular footings.

Levin (1955) presented an upper-bound solution for the problem of the indentation of a smooth circular punch on a half-space of a perfectly plastic material that obeys Tresca's yield criterion. In this solution, the geometry of Hill's plane strain mechanism (Hill, 1950) was used to simulate continuous axisymmetric displacements. Shield (1955a) presented a complete solution for a smooth circular footing on a purely cohesive soil, and Eason & Shield (1960) extended the same solution to the case of a perfectly rough footing. Cox *et al.* (1961) solved a number of cases of the circular surface footing on c–ϕ weightless soil. Cox (1962) extended these solutions by including the soil weight. Houlsby & Wroth (1983), Kusakabe *et al.* (1986) and Tani & Craig (1995) considered the bearing capacity problem of a circular footing on cohesive soil whose undrained strength varies with depth. Shield (1955b) presented upper- and lower-bound solutions for the average bearing pressure at failure of a circular footing on a semi-infinite layer of elastic-perfectly plastic cohesive soil resting on a rough rigid base. Chen (1975) solved the problem of indentation of a circular cylinder of finite dimensions by a flat-ended rigid circular footing.

Butterfield & Harkness (1971) considered the stepped mobilisation of shear strength in rigid plastic Mohr–Coulomb material under strip loading. Shear strain is assumed to be concentrated in the slip lines, and the soil is modelled as rigid until the instant it yields completely. Although this technique was able to calculate the proportional displacement within the plastic mechanism, it was unable to relate ground displacement to shear strain in the soil. In current design practice a reduction factor on peak strength of the soil is introduced to account for the need to predict displacement. However, it is not possible to relate the shear strain (based on the reduced strength mobilisation) to ground displacement other than empirically.

Linear elasticity is often used to calculate displacements.

Manuscript received 17 August 2004; revised manuscript accepted 27 April 2005.
Discussion on this paper closes on 1 February 2006, for further details see p. ii.
* Schofield Centre, Department of Engineering, University of Cambridge, UK.

However, the stress–strain behaviour of soil is highly non-linear from very small strains (Jardine *et al.,* 1984; Burland, 1989; Houlsby & Wroth, 1991). The finite element analyses conducted by Bolton & Sun (1991) for centrifuge tests on a bridge abutment showed the importance of using a non-linear elasto-plastic model in order to predict properly the displacements and stresses on the abutment. Jardine *et al.* (1986) showed that the non-linearity of stress–strain behaviour has a dominant influence on the form and scale of the displacement distribution around shallow foundations.

Bolton & Powrie (1988) and Osman & Bolton (2004) proposed a new design approach for retaining walls based on the theory of plasticity and the mobilisable soil strength concept. The proposed design method treats a stress path in a representative soil zone as a curve of plastic soil strength mobilised as strains develop. Strains are entered into a simple plastic deformation mechanism to predict boundary displacements. Hence the proposed mobilisable strength design (MSD) method can satisfy both safety and serviceability in a single step of calculation. This paper presents an MSD solution for the bearing capacity problem of a shallow circular footing in undrained conditions.

PLASTIC DEFORMATION MECHANISM FOR CIRCULAR FOUNDATIONS

This solution is based on plasticity theory. However, instead of a rigid perfectly plastic material, which is generally used in simple plastic analyses, strain-hardening behaviour is incorporated. In this solution, the ground displacement is related to shear strain in the soil. The key advantage of this technique is that the settlements of circular footings can be predicted directly from the stress–strain data of a triaxial test on a characteristic soil sample. This solution therefore provides a rational procedure for selecting design parameters, because the strength that limits the ground deformation is chosen with respect to the stress–strain behaviour of the soil and the level of acceptable deformations under working conditions.

The well-known Prandtl mechanism (Fig. 1) for plane strain indentation is used first, but only to create a boundary for the continuous displacement field that is taken to exist beneath a circular punch. Within this boundary there are three zones of distributed shear. These regions are required to shear and deform compatibly and continuously with no relative sliding at their boundaries. Strains and compatible displacements are developed according to the stress increment and equilibrium condition. Outside this region, the soil is taken to be rigid. This represents the rapid increase of soil stiffness away from the near-field plastic deformation.

It is possible to satisfy compatibility by considering the kinematics of each of the three soil zones.

Figure 2 shows the active zone OAF. If there is no volume change, the following condition should be satisfied

$$\frac{\partial u}{\partial r}+\frac{u}{r}+\frac{\partial v}{\partial z}=0 \tag{1}$$

where u and v are the radial and vertical displacement respectively, r is the radial distance from the centreline of the footing, and z is the depth below the ground surface.

Axisymmetry conditions imply that $u = 0$ at $r = 0$. If the variation of v is independent of r, then the radial displacement u can be given by

$$u=-\frac{r}{2}\left(\frac{\partial v}{\partial z}\right) \tag{2}$$

The vertical displacement v might be assumed to be given by

$$v=a_1z^2+a_2z+a_3 \tag{3}$$

where a_1, a_2 and a_3 are constants.

Here, v has a maximum value of δ at $z = 0$ and decreases to zero at $z = D/2$. If displacements in the adjoining fan zone are assumed to have no radial component with respect to the fan centre, and if there is no slippage between the zones, then tangential displacement along the boundary OF in the active zone must be zero.

Therefore the radial and vertical components of displacements in the active zone can be given by

$$u=\frac{-4\delta}{D^2}zr+\frac{2\delta}{D}r \tag{4}$$

$$v=\frac{4\delta}{D^2}z^2-\frac{4\delta}{D}z+\delta \tag{5}$$

In each of the remaining zones, the soil is assumed to move

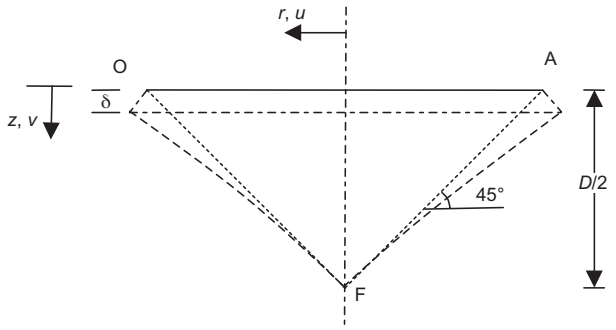

Fig. 2. Active zone OAF

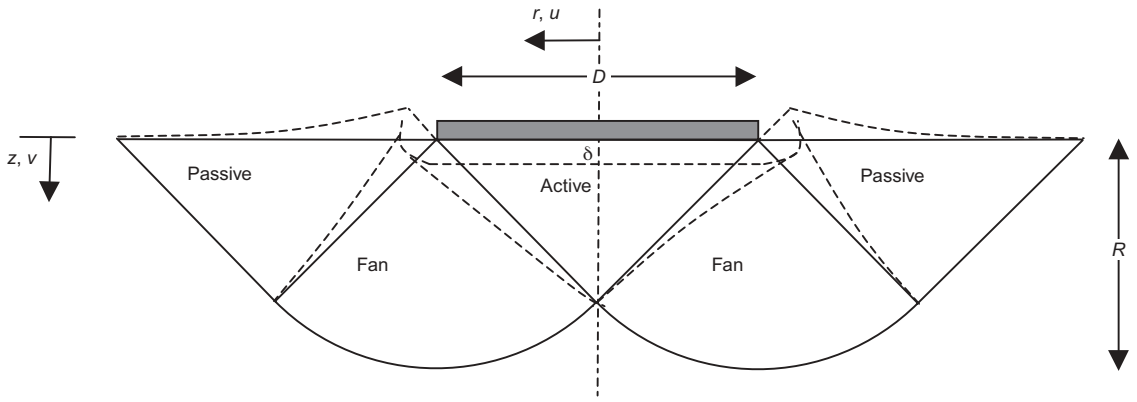

Fig. 1. Plastic deformation mechanism for shallow circular foundation on clay

along lines parallel to the outer rigid boundary (Fig. 3) with displacements decaying with $1/r$ in order to satisfy the incompressibility condition. Table 1 shows the components of the displacement in each zone.

Determination of strains

Strains can be found from the first derivative of displacements. Applying axisymmetric conditions

$$\begin{aligned} \varepsilon_r &= -\frac{\partial u}{\partial r} \quad \gamma_{r\theta} = 0 \\ \varepsilon_\theta &= -\frac{u}{r} \quad \gamma_{\theta z} = 0 \\ \varepsilon_z &= -\frac{\partial v}{\partial z} \quad \gamma_{zr} = -\frac{\partial v}{\partial r} - \frac{\partial u}{\partial z} \end{aligned} \tag{6}$$

The principal strains are given by

$$\begin{aligned} \varepsilon_1 &= \tfrac{1}{2}\left(-\varepsilon_\theta + \sqrt{\varepsilon_\theta^2 + \gamma_{rz}^2 - 4\varepsilon_r\varepsilon_z}\right) \\ \varepsilon_2 &= \varepsilon_\theta \\ \varepsilon_3 &= \tfrac{1}{2}\left(-\varepsilon_\theta - \sqrt{\varepsilon_\theta^2 + \gamma_{rz}^2 - 4\varepsilon_r\varepsilon_z}\right) \end{aligned} \tag{7}$$

where ε_1 and ε_3 are the major and the minor principal strain respectively, and ε_2 is the intermediate principal strain.

Average shear strain

As all displacements are proportional to the vertical displacement δ of the foundation, and all spatial dimensions are proportional to the diameter D of the foundation, it follows by dimensional reasoning that all strain components are proportional to δ/D.

The engineering shear strain ε_s can be defined as the difference between the major and minor principal strains (equation (7))

$$\varepsilon_s = |\varepsilon_1 - \varepsilon_3| \tag{8}$$

The average shear strain mobilised in the deforming soil can be calculated from the spatial average of the shear strain in the whole volume of the deformation zone (Fig. 1). This procedure gives

$$\varepsilon_{s,mob} = \frac{\int_{vol} \varepsilon_s \, dvol}{\int_{vol} dvol} = M_c \frac{\delta}{D} \tag{9}$$

in which M_c can be shown to take the value of 1·35 (Osman, 2005).

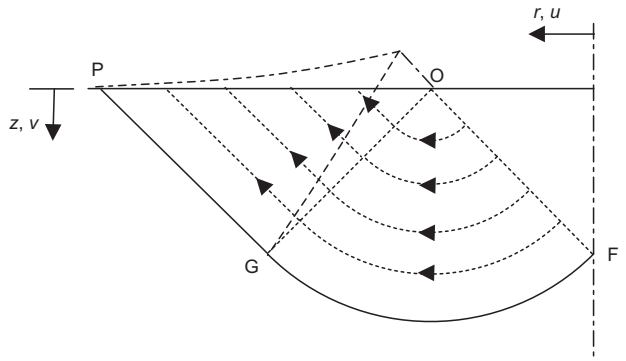

Fig. 3. Displacement field in the fan and passive zones

Hypothesis

The displacement pattern beneath circular footings is idealised by the plastic deformation mechanism shown in Fig. 1. This displacement field links the average shear strain mobilised in the soil, $\varepsilon_{s,mob}$, to the normalised footing settlement δ/D (equation (9)). The shear stresses in the soil are related to the external loading of the footing by the usual bearing capacity coefficient (N_c)

$$\sigma_{mob} = N_c c_{mob} \tag{10}$$

where σ_{mob} is the average applied bearing pressure, and c_{mob} is the shear stress mobilised in the soil.

A relation between applied bearing pressure and the displacement of the footing can be established if the relation between shear stresses and shear strains can be obtained, such as from a carefully chosen undrained triaxial test.

The compromise of the new approach is therefore to couple together an equilibrium solution based on the mobilisation of a *constant* shear stress, c_{mob}, with a kinematic solution based on the creation of an *average* mobilised shear strain, $\varepsilon_{s,mob}$. Fig. 4 illustrates the method of estimating the load–settlement curve directly from a stress–strain curve. This makes it clear that the non-linearity of the representative stress–strain curve is to be taken as identical to that of the *normalised* load–displacement curve of the foundation. Plasticity theory is used to obtain the linear transformation of the axes through the normalisation factors M_c and N_c.

Of course, in a real footing problem, soil elements would differ in their past stress history, and in their response to different stress paths induced by the new loading. Different elements would have different non-linear stress–strain responses and

Table 1. Displacement field for shallow foundation on clay

Zone	Radial displacement, u	Vertical displacement, v
Active zone	$\frac{-4\delta}{D^2} zr + \frac{2\delta}{D} r$	$\frac{4\delta}{D^2} z^2 - \frac{4\delta}{D} z + \delta$
Fan zone	$\frac{V_1 r_1}{r} \frac{z}{\sqrt{\left(\frac{D}{2} - r\right)^2 + z^2}}$	$\frac{V_1 r_1}{r} \frac{\left(\frac{D}{2} - r\right)}{\sqrt{\left(\frac{D}{2} - r\right)^2 + z^2}}$
Passive zone	$\frac{1}{\sqrt{2}} \frac{V_2 r_2}{r}$	$-\frac{1}{\sqrt{2}} \frac{V_2 r_2}{r}$

$$V_1 = 4\sqrt{2}\left(\frac{r_1}{D}\right)^2 \delta, \; r_1 = \frac{D}{2} - \frac{1}{\sqrt{2}}\sqrt{\left(\frac{D}{2} - r\right)^2 + z^2}, \; V_2 = 4\sqrt{2}\left(\frac{r_2}{D}\right)^2 \delta, \; r_2 = \frac{3D}{4} - \frac{r}{2} - \frac{z}{2}$$

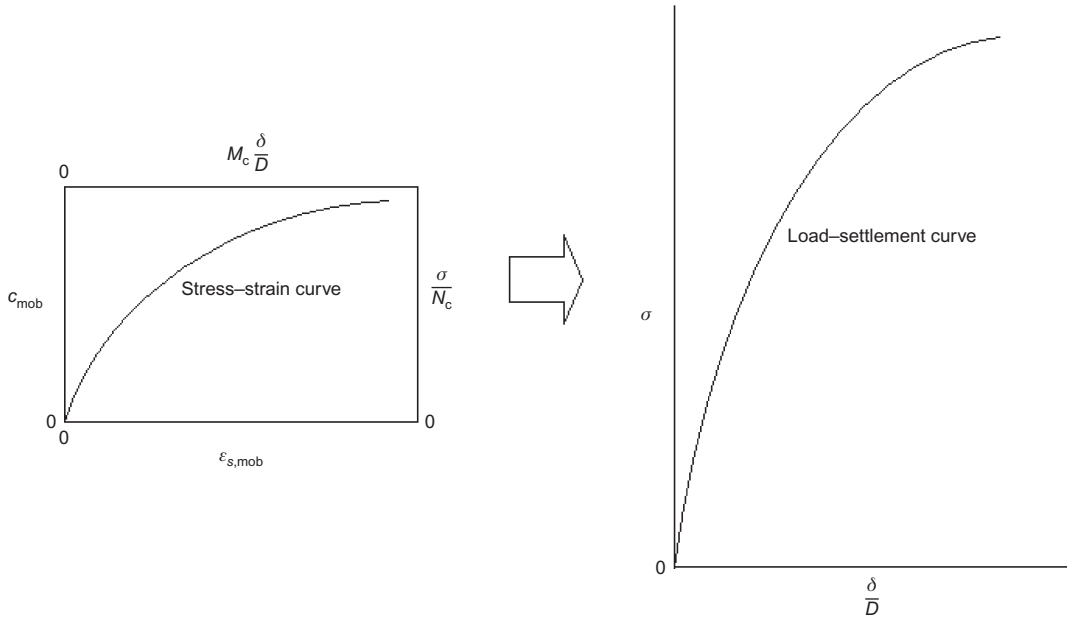

Fig. 4. Calculation procedure in the MSD method

would mobilise different shear stresses. Nevertheless, for the purpose of obtaining a simple calculation, it was considered best to employ a unique representative stress–strain curve. A weighted average approach is adopted to select a representative shear strain that mobilises the required shear strength. The usefulness of this hypothesis will be demonstrated in the following sections.

Consistency of the proposed plastic deformation mechanism

To demonstrate the plausibility of the chosen mechanism, limit analysis calculations will now be carried out using the proposed displacement field to derive an upper bound to the collapse load, taking the soil to be ideally plastic with constant strength c_u. The results are to be compared with existing plasticity solutions.

For a Tresca material, the upper-bound calculation is calculated from the following equation (Shield & Drucker, 1953)

$$\sigma \frac{\pi}{4} D^2 \dot{\delta} = \dot{W} = \dot{D} = 2\int_{vol} c_u |\dot{\varepsilon}_1| \, \mathrm{d}vol + \int_s c_u |\Delta v| \mathrm{d}s \qquad (11)$$

where $\dot{W}$ is the work done by the vertical load σ on the footing, $\dot{\delta}$ is the downward incremental displacement of the footing, $\dot{D}$ is the total energy dissipation, c_u is the undrained shear strength, s is the surface domain, Δv is the jump in displacement increment across the discontinuity, and $\dot{\varepsilon}_1$ is the largest principal plastic strain increment.

As the distributed shear zones in Fig. 1 have been proved to shear and deform compatibly and continuously with no relative sliding at their boundaries, there is no displacement discontinuity. Accordingly,

$$\int_s c_u |\Delta v| \mathrm{d}s = 0$$

The largest principal plastic strain increment $\dot{\varepsilon}_1$ can be calculated from the displacement increments at collapse following equations (7) and (8) rewritten in terms of incremental plastic strains and incremental displacements at collapse. As is the case with the classical solutions, with which a comparison will shortly be made, changes of overall geometry due to finite deformation will be ignored.

The bearing capacity factor N_c is calculated by equating the energy dissipation and the work done. The N_c value calculated using this technique for a smooth circular footing is 5·86. The computation is detailed in Osman (2005). This value is only 3% higher than that calculated by Shield (1955a) and Houlsby & Wroth (1983), which was 5·69. Although this close correspondence cannot be taken as proof that the selected displacement field is adequate, its consistency is encouraging. It must, however, be recognised that alternative plastic mechanisms have been proposed by others seeking solutions to the bearing capacity of circular foundations. For example, Kusakabe *et al.* (1986) followed Levin (1955) in adapting Hill's (1950) plane strain mechanism for solution in axial symmetry. Although Levin's solution offers $N_c = 5{\cdot}84$ for the bearing capacity of a smooth circular punch, which is slightly better than the authors' solution of 5·86, Levin's displacement field (Fig. 5) gives zero displacement at every point beneath the centreline of the footing, which seems physically unreasonable. The selection of a mechanism that is adequate to represent both equilibrium and kinematics can be taken only following an independent verification using finite element analysis.

COMPARISON WITH FINITE ELEMENT (FE) ANALYSIS

A series of axisymmetric finite element analyses has been performed to predict the displacement of a circular footing in the short term in which undrained soil conditions are assumed. Accordingly, excess pore pressure is not allowed to

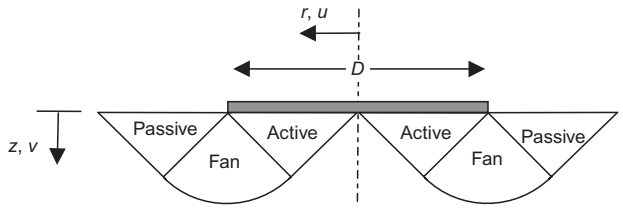

Fig. 5. Levin's mechanism for shallow smooth circular foundation on clay

dissipate during the analysis. In the finite element simulation, the Strain Dependent Modified Cam Clay (SDMCC) soil model (Dasari & Britto 1995; Dasari, 1996) was used. The analyses were carried out using ABAQUS/STANDARD version 6·2 software (Hibbit, Karlsson & Sorensen Inc., 2001).

The Strain Dependent Modified Cam Clay (SDMCC) soil model

The SDMCC soil model can simulate the variation of stiffness with strain and the development of hysteresis inside the Modified Cam Clay (MCC) yield surface, which controls large-strain behaviour through the MCC flow rule.

Figure 6 shows a typical variation of shear modulus in SDMCC. At very small strain ($<10^{-5}$) the tangent shear modulus G is constant for any given overconsolidation ratio (OCR) and mean normal stress p', and is given by

$$G_{\max} = Ap'^{n_1}\mathrm{OCR}^{m_1} \tag{12}$$

where A, n_1 and m_1 are constants.

At small strains ($10^{-5} < \varepsilon_q < 10^{-2}$) the tangent shear modulus is taken to be in the form of

$$G = Bp'^{n_2}\mathrm{OCR}^{m_2}\varepsilon_q^{b_2} \tag{13}$$

where B, n_2, m_2 and b_2 are constants.

Unloading–reloading loops are modelled by Masing's rule

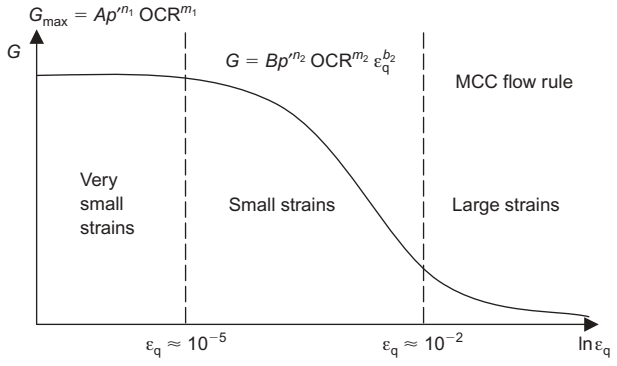

Fig. 6. Typical variation of soil stiffness with strain in SDMCC soil model

(Masing, 1926). The stiffness–strain curve during the subsequent unloading and reloading is given by

$$G = Bp'^{n_2}\mathrm{OCR}^{m}\left(\frac{\varepsilon_{\mathrm{rev}} - \varepsilon_q}{2}\right)^{b_2} \tag{14}$$

where $\varepsilon_{\mathrm{rev}}$ is the reference strain corresponding to the point of the last reversal and ε_q is the current deviatoric strain.

Bulk modulus is a function of mean normal effective stress (p'), OCR and volumetric strain (ε_v)

$$K_{\max} = Cp'^{n_3}\mathrm{OCR}^{m_3} \tag{15}$$

$$K = Cp'^{n_4}\mathrm{OCR}^{m_4}\varepsilon_v^{b_4} \tag{16}$$

where C, n_3, m_3, D, n_4, m_4 and b_4 are constants. The derivation of the various parameters was explained by Dasari (1996) and Bolton *et al.* (1994).

Table 2 lists the 19 soil parameters used in the analysis. These parameters are selected to fit a typical triaxial stress–strain curve of undisturbed London Clay (Fig. 7).

The FE mesh

The soil was modelled using eight-node axisymmetric consolidation elements. The mesh domain was sufficiently large to eliminate boundary effects so that the changes in stresses and displacements remote from the footing were negligible. The footing was taken to be rigid and smooth. Smaller elements were used near the footing where the changes of stresses and strains are significant. The bottom boundary was restrained from both horizontal and vertical movements, and the left- and right-hand boundaries were restrained horizontally. Details of the finite element mesh are shown in Fig. 8.

In situ *conditions*

The stress history of the soil was assumed to comprise one-dimensional consolidation followed by the removal of an effective overburden pressure of 1100 kPa to create a heavily overconsolidated clay. The lateral earth pressure coefficient at rest (K_0) up to the passive limit is then calculated using the following equation (Mayne & Kulhawy, 1982)

$$K_0 = K_{\mathrm{nc}}\mathrm{OCR}^{\sin\phi} \tag{17}$$

where ϕ is the critical state angle of friction of the soil

Table 2. Parameters for SDMCC soil model

Slope of one-dimensional compression line in v–lnp' space, λ	0·161
Slope of unload–reload line in v–lnp' space, κ	0·062
Slope of critical state line in q–p' space, M	0·89
Void ratio on critical state line at $p' = 1$ kPa, e_{cs}	1·45
Poisson's ratio, ν	0·2
Parameters for shear modulus	
A	319
n_1	1·0
m_1	0·2
B	5·6
n_2	1·0
m_2	0·2
b_2	−0·362
Parameters for bulk modulus	
C	304
n_3	1·0
m_3	0·2
D	1·147
n_4	1·0
m_4	0·2
b_4	−0·488

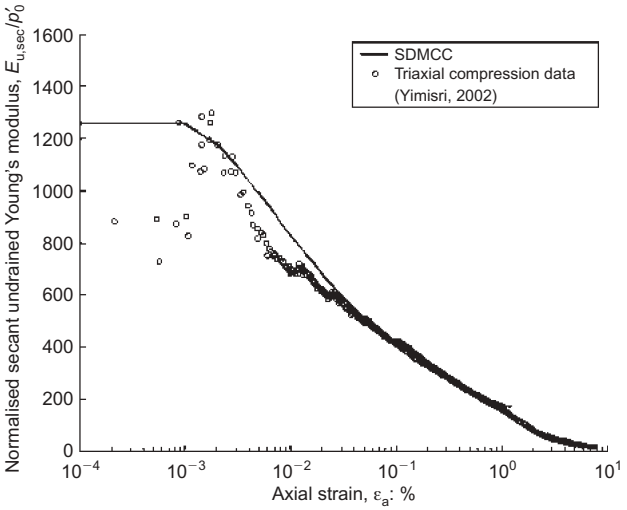

Fig. 7. Stiffness data of London clay fitted by SDMCC model

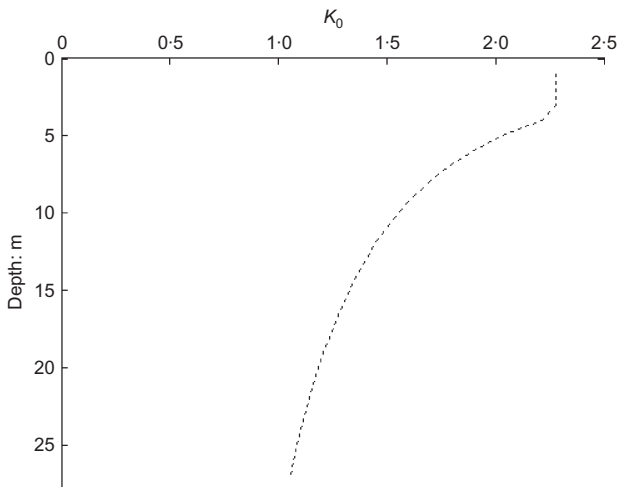

Fig. 9. K_0 profile adopted in London clay

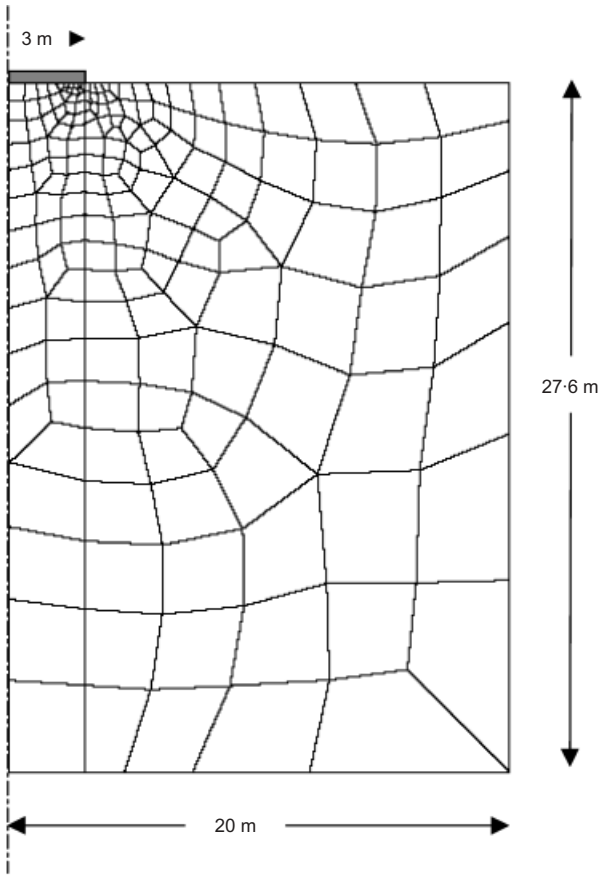

Fig. 8. Finite element mesh for analysis of circular footing

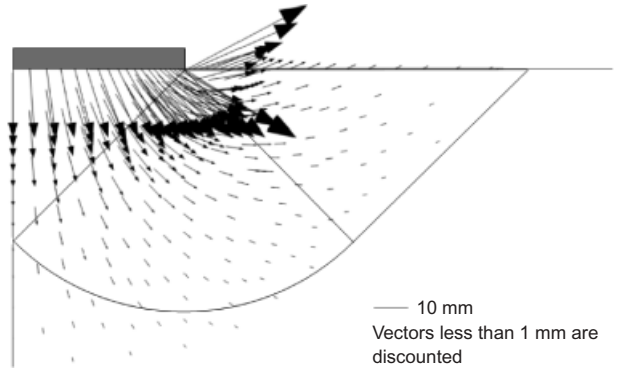

Fig. 10. Displacement vectors at a footing bearing pressure of 100 kPa

($\phi = 22{\cdot}8°$ in this FE simulation). K_{nc} is the coefficient of earth pressure for normally consolidated soil and is assumed to be given by Wroth's empirical method (Wroth, 1975)

$$K_{nc} = 1 - \sin\phi \tag{18}$$

The K_0 profile thereby derived is shown in Fig. 9. The water table was taken at the ground level.

Results of SDMCC analysis

Figure 10 shows soil displacement vectors at a footing carrying a bearing pressure σ of 100 kPa. This figure shows that significant soil movement occurred mainly within the boundary of the Prandtl mechanism, so that the proposed plastic deformation mechanism of Fig. 1 can reasonably approximate the deformation pattern beneath the smooth circular footing in the FE analysis. In comparison, Levin's (1955) mechanism shown in Fig. 5 is clearly unsuitable for predicting displacements, even though it was acceptable for predicting collapse loads.

It is well known that in soil there is no unique relationship between strains and stresses. The stress–strain relation in soil is complicated, and subject to many factors such as stress history due to loading, unloading and reloading procedures (Atkinson *et al.*, 1990; Wood, 1990; Viggiani & Atkinson, 1995). The proposed plastic deformation mechanism discussed earlier was derived for a material with constant c_u value and a unique stress–strain relation. In this finite element validation, Fig. 11 shows the variation of the *in situ* shear modulus with depth and the undrained strength profile of the simulated London clay. Ideally, the geometry of the deformation mechanism should be optimised according to the rate of increase of shear strength with depth (Houlsby & Wroth, 1983; Kusakabe *et al.*, 1986; Tani & Craig, 1995), and consequently the compatibility factor M_c should vary. The following validation will demonstrate that a simpler approach is sufficiently accurate. A soil element at some characteristic depth will be selected to provide the representative stress–strain relation and the constant c_u value to be used in the assumed zone of plastic deformation. The representative location beneath a pad of diameter D is taken in MSD to be at $0{\cdot}3D$, close to the centroid of the plastic deformation zone at $0{\cdot}273D$. This location is marked in Fig.

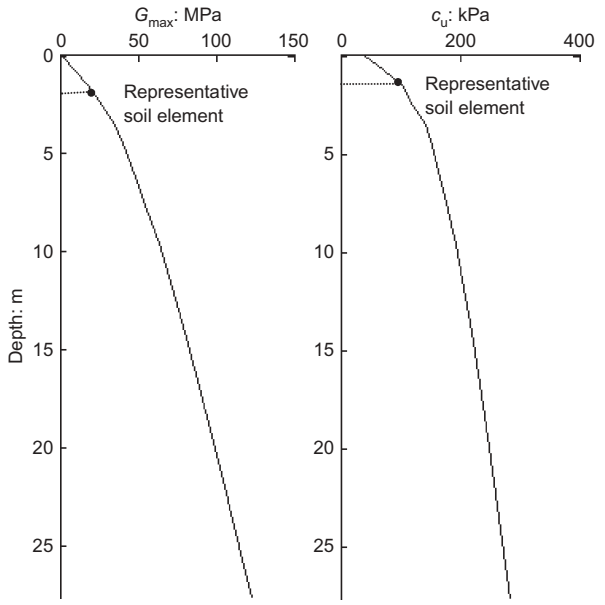

Fig. 11. Variation of *in situ* soil stiffness and undrained shear strength with depth

11, making it clear that the FE simulation refers to site conditions in which soil strength and stiffness increase markedly with depth.

An FE simulation of an undrained triaxial test with a stress history identical to that of an element at depth $0{\cdot}3D$ (i.e. 1·8 m) in Fig. 8 was used to plot the representative stress–strain curve. This FE simulation would be replaced in practice by the triaxial data of undisturbed samples or by a pressuremeter test. Fig. 12 shows the representative stress–strain curve used in the MSD calculations.

The MSD calculation process, for comparison with the FE procedure, is set out below.

Suppose that a smooth circular footing of diameter $D = 6$ m is loaded vertically with 100 kPa. Then the change in mobilised shear stress Δc_{mob} is

$$\Delta c_{\mathrm{mob}} = \frac{\sigma_{\mathrm{mob}}}{N_{\mathrm{c}}} = \frac{100}{5{\cdot}69} = 17{\cdot}57 \text{ kPa}$$

Considering axial symmetry, the change in mobilised deviatoric stress is twice the change in shear stress

$$\Delta q_{\mathrm{mob}} = 2 \times 17{\cdot}57 = 35{\cdot}15 \text{ kPa}$$

From the stress–strain curve (Fig. 12) the corresponding axial strain in the undrained compression test is 0·25%. The

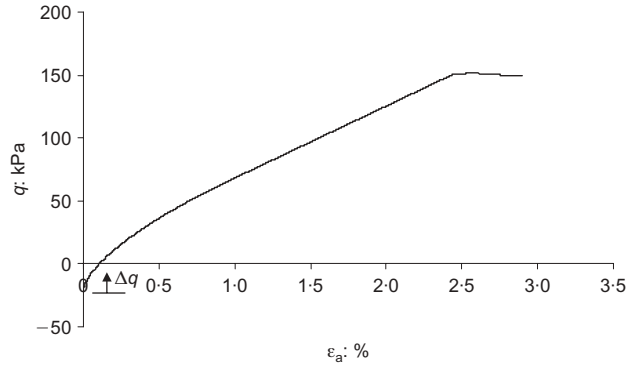

Fig. 12. Representative stress–strain curve for *in situ* London clay

engineering shear strain ε_s is equal to 1·5 times the axial strain ε_a.

Thus

$$\varepsilon_s = 1{\cdot}5\varepsilon_a = 1{\cdot}5 \times 0{\cdot}25\% = 0{\cdot}375\%$$

From the plastic deformation mechanism (equation (9)), the immediate settlement δ can be calculated as follows

$$\delta = \frac{\varepsilon_s D}{1{\cdot}35} = \frac{0{\cdot}00375 \times 6000}{1{\cdot}35} = 17 \text{ mm}$$

Figure 13 shows a comparison between MSD calculations and FE predictions for footing bearing pressure up to 240 kPa. The MSD calculations were based on stress–strain data from an undisturbed soil sample taken at a depth of $0{\cdot}3D$ of the deformation mechanism. This figure shows that the straightforward MSD calculations fall within 10% of the FE analysis throughout.

Figure 14 shows MSD calculations based on stress–strain curves obtained from 'samples' at various depths compared with the FE analysis. This figure confirms that stress–strain data from an undisturbed soil sample taken at a characteristic depth of $0{\cdot}3D$ can best be used in the prediction of undrained settlement of a shallow foundation on soil with the particular stress–strain characteristics used in this FE

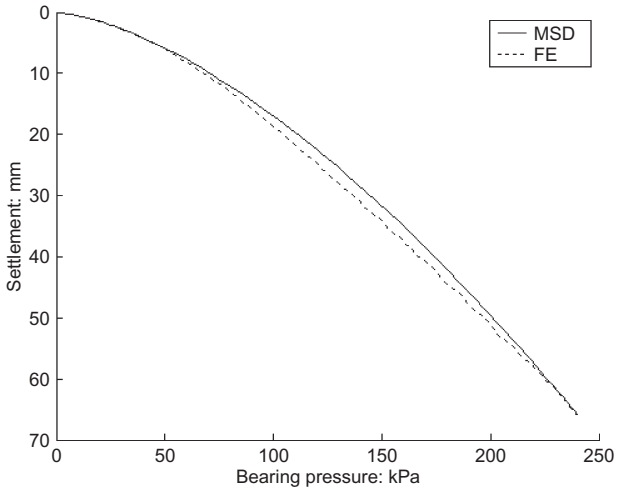

Fig. 13. Comparison between MSD and FE predictions for footing settlement on London clay

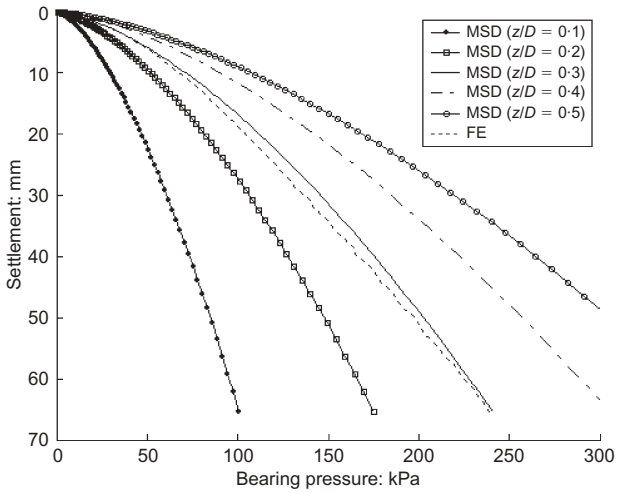

Fig. 14. Influence of selected representative depths on MSD predictions

validation. Further validation, using the published evidence from field studies, will be undertaken in the next section.

These FE analysis results have shown clearly that the MSD approach captures the effects of the non-linear non-homogeneous soil response. It has not been necessary to fit an elastic modulus to the stress–strain behaviour. Indeed, it has not been necessary to fit any mathematical expressions to the raw stress–strain data of the simulated representative sample.

BACK-ANALYSIS OF A LOADING TEST ON A STIFF FOOTING AT BOTHKENNAR

Site location and soil properties

The Bothkennar soft clay test site is a facility for large-scale experimental research. It is owned and managed by the UK government through the Engineering and Physical Science Research Council (EPSRC). It lies approximately midway between Edinburgh and Glasgow, and borders onto the River Forth in Scotland. The site has an area of 11 ha and 20 m depth of soft saturated soils, and has an uncomplicated soil profile, which facilitates back-analysis and the interpretation of field experiments. An extensive site investigation was performed and documented by various authors (Institution of Civil Engineers, 1992). Pad loading tests were carried out by Jardine *et al.* (1995) to investigate bearing capacity and load–displacement behaviour under short-term and long-term conditions.

The soil profile under the pad footings is summarised in Fig. 15, and the undrained strength profile is shown in Fig. 16.

Field tests

Two reinforced concrete pads were cast in 0·8 m deep excavations. Pad A was 2·2 m square and pad B was 2·4 m square. As it is common in bearing capacity calculations to treat circles and squares of equal areas as being equivalent (Skempton, 1951), the equivalent diameters of pad A and pad B are 2·48 m and 2·71 m respectively. However, there is no theoretical justification for this assumption. The aim of test A was to study the short-term behaviour and the ultimate bearing capacity of rigid foundations under vertical loads; the long-term behaviour under maintained load was examined in test B. In this study the settlement of pad A only is compared with MSD prediction.

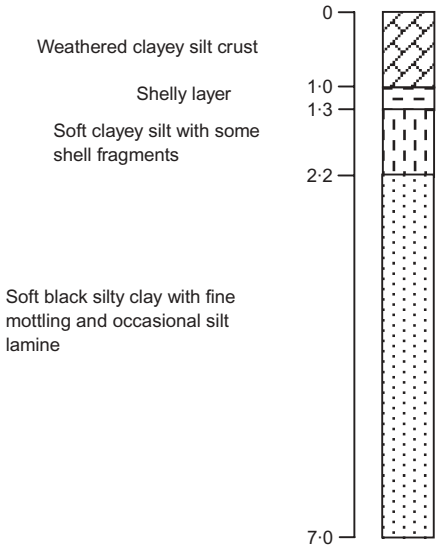

Fig. 15. Soil profile at Bothkennar (after Jardine *et al.*, 1995)

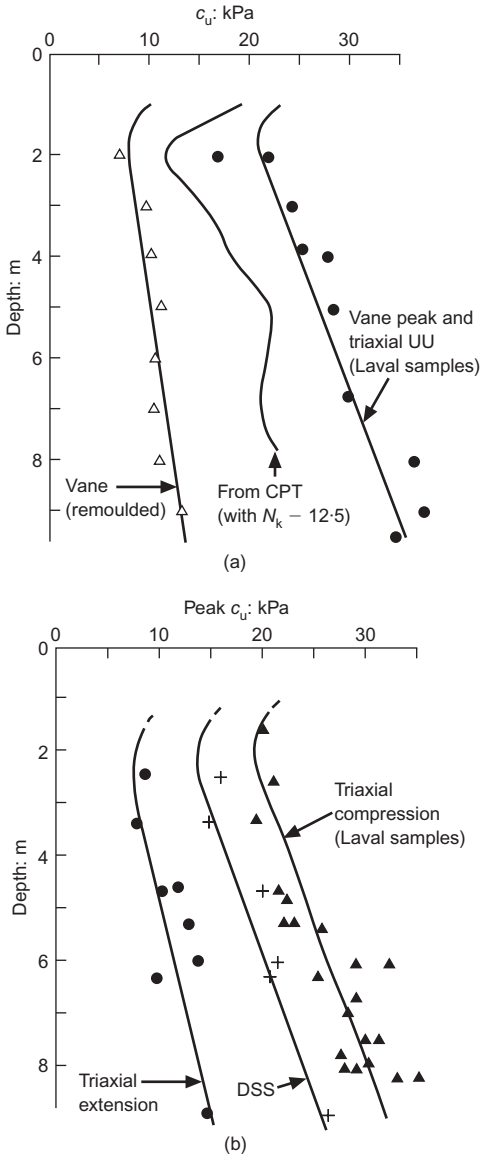

Fig. 16. Undrained strength profiles for Bothkennar clay (Jardine *et al.*, 1995): (a) C_u values from field and unconsolidated-undrained triaxial tests; (b) C_u values from direct simple shear tests and anisotropically consolidated undrained triaxial tests

Pore water pressure dissipation during loading

Jardine *et al.* (1995) compared the pore pressure measured under the centreline of pads A and B with the results of non-linear FE analysis, and concluded that that the upper silty strata ($z/D < 0{\cdot}5$) showed pore water pressure dissipation during loading pause periods. However, the conditions were practically undrained on the centreline beneath $z/D = 0{\cdot}5D$. The constitutive model used in this comparison (the LPC2 model of Jardine *et al.*, 1986), does not account for anisotropy, sensitivity or layering of the natural soils.

The field dissipation rate invariably slows dramatically once large-strain yield stresses are exceeded (Jardine *et al.*, 1995).

Surface settlement during loading

Figure 17 shows the profile of ground surface settlement measured during loading to failure. The bearing pressure is represented in terms of the mobilised load factor L_f, which is defined as the ratio of current bearing pressure to the ultimate capacity found in test A. These load factors were

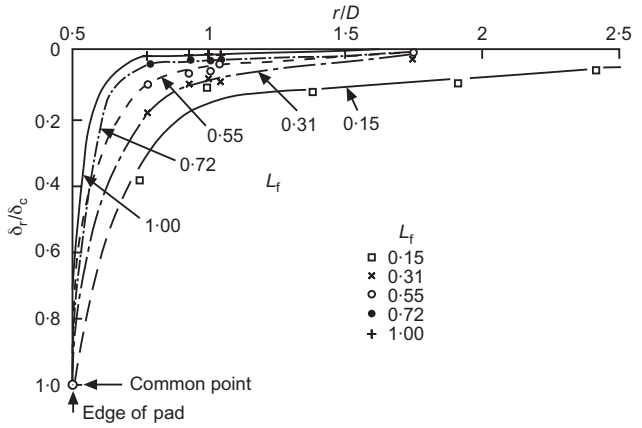

Fig. 17. Surface settlement profile at a range of load factors (Jardine *et al.*, 1995)

plotted with axes r/D and δ_r/δ_c (ratio of radial distance from the centre of the footing to its diameter, and ratio of soil settlement to the settlement of the pad's centre point, respectively). The ground surface displacement appears to diminish rapidly with radial distance, as anticipated by the proposed plastic deformation mechanism shown in Fig. 1. However, settlement rather than heave was observed adjacent to the pad. If this observation can be relied upon, it might arise from partial drainage in the upper soil layers.

MSD calculations

Assumptions. The behaviour of Bothkennar clay may be described at various levels of sophistication. However, the MSD method aims to provide a simplified model of the complex reality for use in design and decision-making. The approximation should be good if the mechanism is appropriate; overall function is more important than local details. The following assumptions have been made in the back-analyses of the pad footing tests using the MSD method.

(*a*) The soil is laterally homogeneous and vertically consistent, although it is permitted a vertical profile of strength and stiffness dictated by variable over-consolidation ratios.
(*b*) The average shear stress induced in the zone of deformation is deduced from standard bearing capacity coefficients applied to estimate working loads.
(*c*) The displacements are controlled by the average soil stiffness in the zone of the deformation, through the assumption of a plastic deformation mechanism and the selection of a representative stress–strain curve.

The plastic deformation mechanism in the MSD method is derived for a surface footing. However, the pad footing at Bothkennar is embedded at a depth of 0·8 m ($z/D = 0{\cdot}32$). Brinch Hansen's (1970) depth correction factor f_d was adopted to account for embedded depth z in the calculation of the mobilised strength in MSD of a foundation of width D. The bearing capacity factor N_c should be increased by factor f_d.

$$f_d = 1 + \frac{0{\cdot}4z}{D} \tag{19}$$

For back-analysis of pad A the correction factor f_d of 1·13 was accordingly adopted. The bearing capacity factor for a rough circular surface is 6·05 (Eason & Shield, 1960); applying the depth correction factor gives an overall bearing capacity factor N_c of 6·83. No comparable adjustment was made to the plastic deformation mechanism apart from recognising that the representative depth below ground surface should be increased.

Stress–strain behaviour. The representative sample in the MSD calculations should be taken at a depth of $0{\cdot}3D$ below the base, which in this case is about 1·5 m below the ground surface. Although it is routine in design practice to monitor the footing settlement and ground deformations around structures, it is much less common to take representative samples for testing from shallow depths, even when designing footings. Fig. 18(a) shows triaxial compression data for different depths of Bothkennar soft clay, and Fig. 18(b) shows triaxial extension stress–strain data. No triaxial data at the required shallow depth (1·5 m) are reported in the literature. Engineering judgement is therefore needed to estimate stress–strain behaviour at the required characteristic depth. It should be borne in mind that, at the characteristic depth, the peak undrained shear strengths in compression and extension are 20 kPa and 10 kPa respectively (Fig. 15), the soil will be less stiff at shallower depth, and the Sherbrooke sampler produced higher-quality samples than other samples

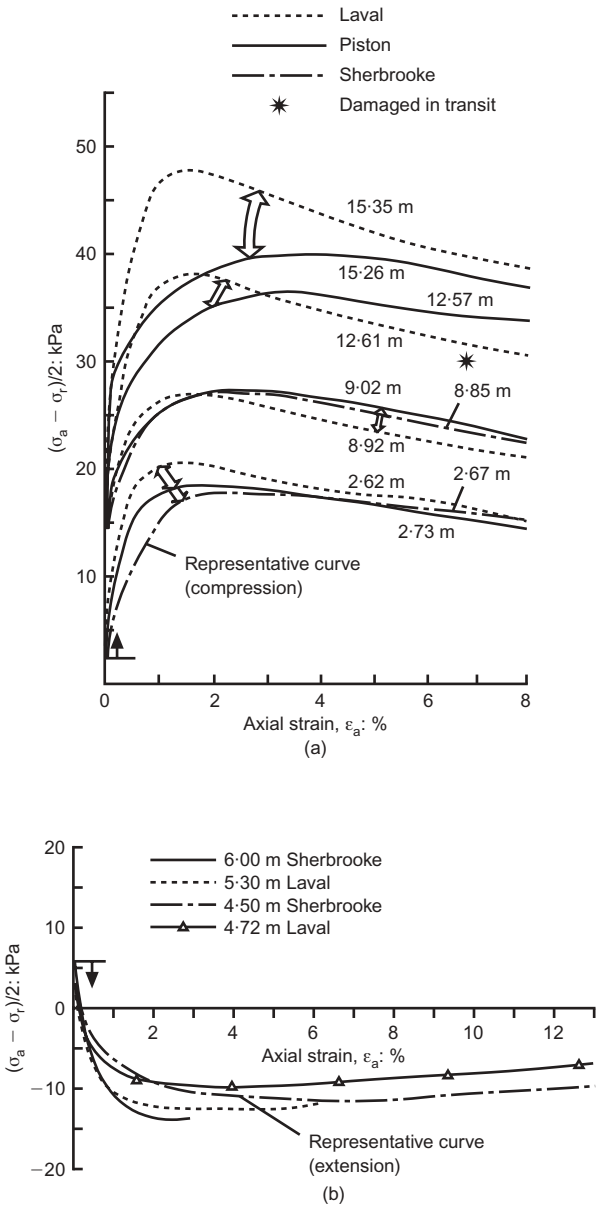

Fig. 18. Soil stress–strain behaviour of Bothkennar clay (after Hight *et al.*, 1992): (a) CK_0U triaxial compression; (b) CK_0U triaxial extension

in Bothkennar soft clay (Hight *et al.*, 1992). These three considerations were used to select the representative stress–strain curves adopted in the MSD calculation and indicated in Fig. 18.

Comparison of the results. Figure 19 shows the MSD calculations compared with the field measurements. Although there is a larger discrepancy at high bearing pressures (possibly due to consolidation as discussed earlier), the results show a good agreement in the prediction of the settlements up to 20 mm. In the MSD method, the deformation is assumed to be controlled by the average soil stiffness. Data of both triaxial compression and extension should be taken into account. Triaxial compression of a vertical core of soil fits the deformation beneath the centreline of the footing. A triaxial extension test only approximately reproduces the rotation in the principal compressive strain direction in the soil outside the footing. In general, the soil deformation does not conform exactly to either, and the designer must decide whether to base a prediction on the average mobilised stress–strain curve or on the lower of the two. Figs 18 and 19 demonstrate that the MSD method places this judgement in the hands of the designer in an extremely transparent fashion.

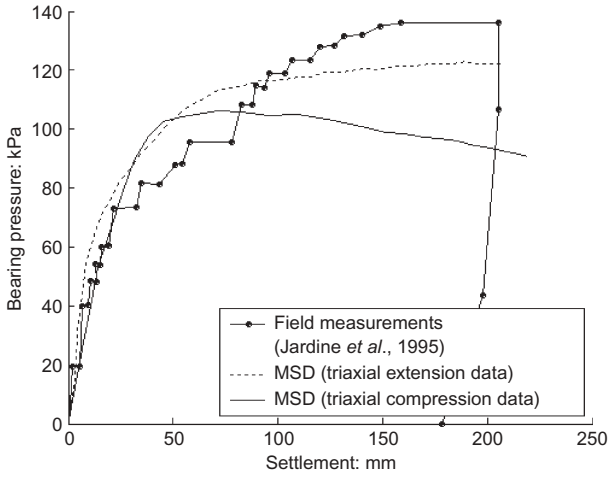

Fig. 19. Comparison between MSD prediction and field measurements for load–settlement curve at Bothkennar

Décourt (1992) proposed that the allowable settlement of a shallow foundation should be taken as 0·75% of the diameter of the loading surface, which gives a settlement of 18·6 mm in the present case. This corresponds to an applied load of 60 kPa. The mobilised undrained shear strength was therefore about 10 kPa, which represents about 50% of the undrained strength c_u measured in compression tests. This example shows that serviceability checks can be more critical than collapse checks. Satisfaction of serviceability limits usually leads to the satisfaction of safety requirements.

BACK-ANALYSIS OF A LOADING TEST ON A RIGID FOOTING AT KINNEGAR

Ground conditions

The field experiment on a vertically loaded shallow foundation at the Kinnegar site reported by Lehane (2003) has been back-analysed using the MSD method. The Kinnegar site is located on the south side of Belfast Lough in Northern Ireland.

Figure 20 shows that the soil conditions in the vicinity of the footing test at Kinnegar comprise ∼1 m of topsoil and fill followed by a thin (0·75 m) deposit of sandier estuarine soil overlying soft estuarine clayey silt, which is known locally as sleech, to a depth of approximately 8·5 m. The water table was at a depth of 1·4 m. The base of the footing was located at a depth of 1·6 m below the ground surface.

Figure 21 shows the results of anisotropically consolidated undrained triaxial compression and extension tests for samples taken from between 4·5 m and 4·8 m depth reported by Lehane (2003).

MSD calculations

In the MSD calculations the square footing is treated as a circular footing of equivalent area, with a diameter of 2·26 m. The footing is treated as a rough footing in the MSD calculations. Following Eason & Shield (1960), the bearing capacity factor N_c for a rough circular pad is taken to be 6·05. Applying Brinch Hansen's (1970) depth correc-

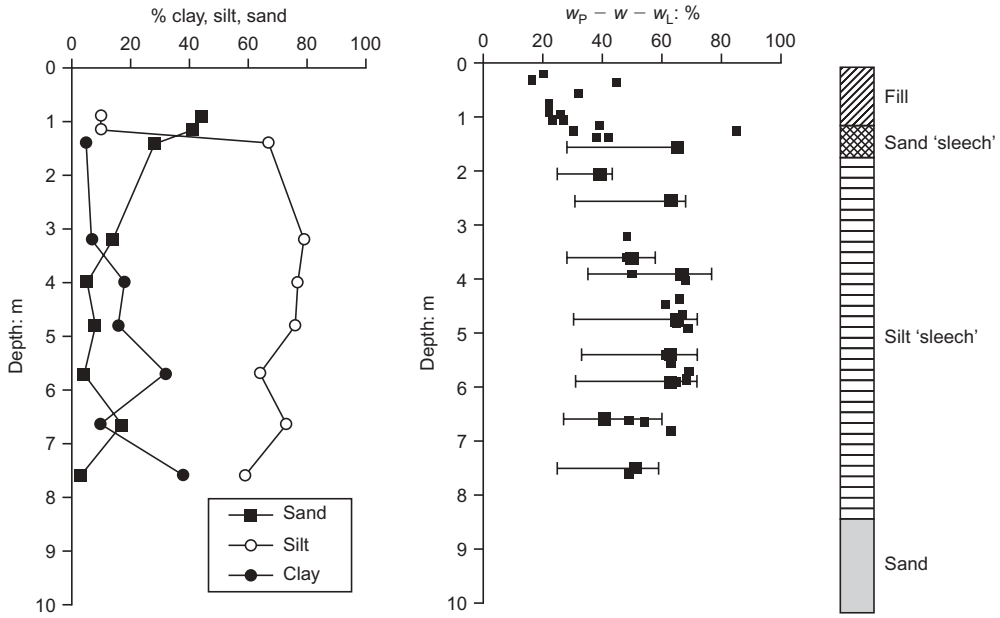

Fig. 20. Classification data for Kinnegar (from Lehane, 2003)

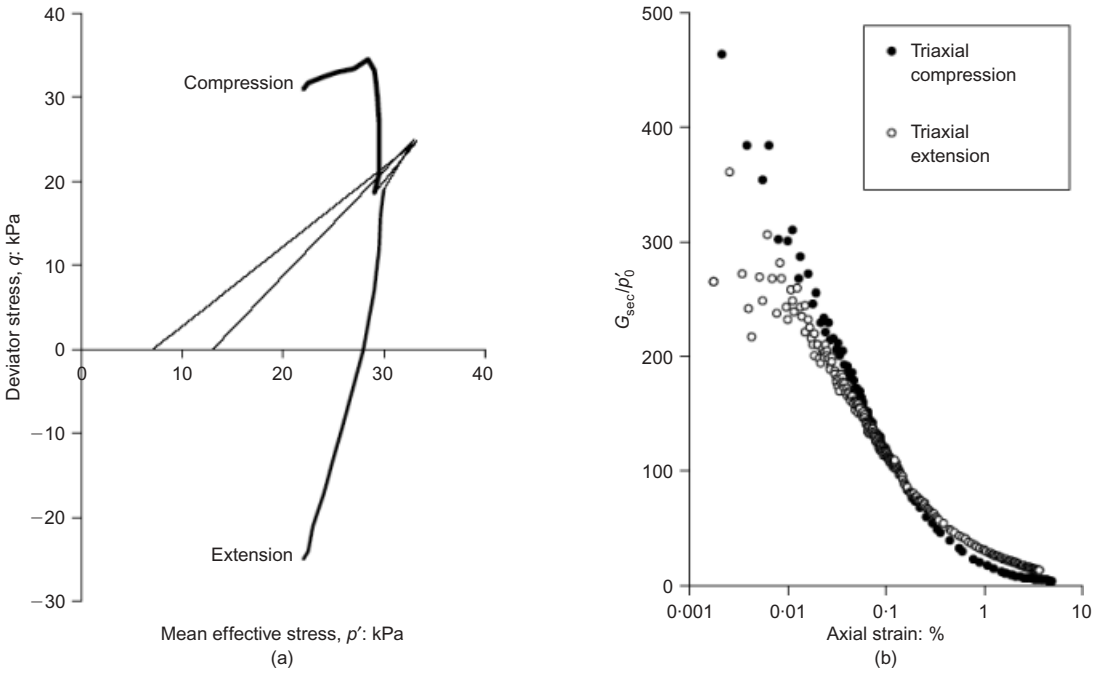

Fig. 21. Stress–strain data for Kinnegar (from Lehane, 2003): (a) stress path; (b) stiffness–strain data

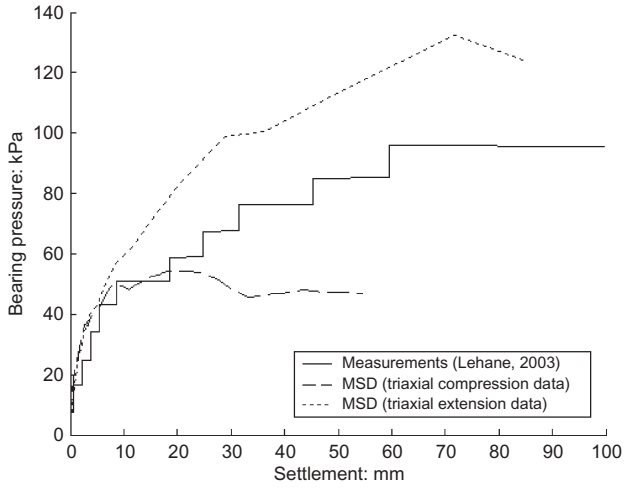

Fig. 22. Comparison between measured and predicted load-settlement response of Kinnegar pad loading test

tion factor (1·28 in this case), the overall N_c value is given as 7·76.

In the MSD method, the characteristic depth is 0·3 times the footing diameter: that is, about 0·68 m measured from the bottom of the footing or 2·28 m below the ground surface. Lehane (2003) estimated that the mean effective stresses p'_0 between depths of 0·5 m and 1·75 m below the foundation varied from about 25 ± 5 kPa to 35 ± 5 kPa. Therefore the mean effective stress p'_0 at the characteristic depth is taken to be 25 kPa. The triaxial compression and extension stress–strain data at this stress level were reproduced using the shear modulus data of Fig. 20(b). The deviatoric stress axis is scaled to bearing pressure by dividing the deviatoric stress by 2 to calculate the shear strength mobilised in the soil, which in turn is multiplied by the bearing capacity factor ($N_c = 7{\cdot}76$). The axial strain axis ε_a is scaled to the relative displacement axis by multiplying by 1·5 to obtain the engineering shear ε_s. Then it is divided by 1·35 to obtain settlement diameter ratio (δ/D), as indicated by equation (9).

Figure 22 compares the observed and predicted load–settlement response. Several conclusions can be drawn from this case history.

(*a*) The observed load–settlement curve is non-linear from the earliest stages of loading.
(*b*) Soil anisotropy can have a significant influence on the settlement of shallow foundations on soft clay. The reason for this is that large variations in the inclination of the major principal stress to the vertical occur in the deformed zones directly beneath and adjacent to the footing. Therefore there will be large differences in the mobilised undrained strengths beneath the footing.
(*c*) It is important to take account of soil anisotropy observed through laboratory and field experiments if more accurate predictions are to be made of the settlement of shallow foundations on soft clay.
(*d*) MSD calculations that assume isotropic soil behaviour, and use either the triaxial compression or triaxial extension data, offer bounds for the predicted footing settlement. The average load–settlement curve plotted by taking the average values of the calculated settlement based on extension and compression data conforms well to the measured data. Therefore the effect of anisotropy in settlement calculations in the MSD method can apparently be handled simply and rather accurately by taking the average soil stiffness.

CONCLUSIONS

Conventional bearing capacity theory has been extended by including plastic deformation mechanisms with distributed plastic strains. The proposed plastic deformation mechanism uses the well-known Prandtl solution for indentation to set the boundaries of a plastic zone of deformation beneath a circular punch. Within this zone, a continuous displacement field has been imposed to avoid discontinuities and cracks and to satisfy incompressibility. Accordingly, this solution can be used to derive an upper bound to the

collapse load. The feasibility of this mechanism can be judged by the fact that this approach overestimates the penetration resistance of a rigid-plastic material by a circular smooth punch by only 3% compared with the published solution widely regarded as correct. The usefulness of this solution, however, is that it can be applied to create an appropriate relation between penetration force and displacement of materials that are strain-hardening. This technique can provide a unified solution for design problems. It offers simple hand calculations, which can give reasonable results for load–settlement behaviour of shallow foundations, when compared with complex FE analyses.

The selection of soil parameters for design is sometimes difficult, because the properties of shallow and deep soil elements are quite different. The selection of a characteristic stress–strain curve is obviously necessary in design, but is difficult to decide upon. However, for the purposes of designing shallow footings in consistent soils, displacements can be assumed to be controlled by the average soil stiffness in the zone of deformation. Stress–strain data from an undisturbed soil sample taken at the mid-depth of the deformation mechanism, 0·3D below a foundation base of diameter D, can be used to obtain the load–settlement curve of a shallow circular foundation. Calibration against FE analyses demonstrated the accuracy of this approach even when there were significant variations of soil stiffness and strength with depth.

The back-analysis of Bothkennar and Kinnegar loading tests shows that MSD can be used by an engineer to obtain quite accurate estimate of settlements in the serviceability range. They also confirm that serviceability checks can be more critical than collapse checks. Satisfaction of serviceability limits can lead consequently to the satisfaction of safety requirements.

Soil anisotropy can have a significant influence on the settlement of shallow foundations on soft clay. The effect of anisotropy can be handled in the MSD method by taking the average soil stiffness from extension and compression triaxial data, providing a simple prediction that should be sufficiently accurate for practical purposes.

ACKNOWLEDGEMENTS

The authors are grateful to Cambridge Commonwealth Trust and to the Committee of Vice-Chancellors and Principals of UK Universities (Overseas Research Scheme) for their provision of financial support to the first author.

NOTATION

A, B shear modulus parameters in Strain Dependent Modified Cam Clay soil model
b shear exponent in Strain Dependent Modified Cam Clay soil model
C bulk modulus parameter in Strain Dependent Modified Cam Clay soil model
c_u undrained shear strength
c_{mob} mobilised shear strength
D diameter of circular footing
$\dot{D}$ total energy dissipated
e_{cs} void ratio on critical state line at $p' = 1$ kPa
f_d depth correction factor for bearing capacity
K bulk modulus
K_{max} maximum bulk modulus
K_{nc} coefficient of earth pressure for normally consolidated soil
K_o lateral earth pressure coefficient at rest
K_p passive earth pressure coefficient
L_f mobilized load factor
m overconsolidation exponent in Strain Dependent Modified Cam Clay soil model
M slope of critical state line in q-p′ space
M_c compatibility factor
N_c bearing capacity factor
p' mean normal effective stress
q deviatoric stress
q_{mob} mobilised deviatoric stress
r radial distance
s surface domain in energy dissipation calculations
u radial displacement in the plastic deformation mechanism for circular footing
v vertical displacement in the plastic deformation mechanism for circular footing
$\dot{W}$ work done by external loads on the footing
z depth
$\gamma_{r\theta}$, $\gamma_{z\theta}$, γ_{zr} shear strain in r-θ, z–θ and z-r planes respectively
δ settlement of shallow foundation
$\dot{\delta}$ incremental downward displacement of shallow foundation
Δv displacement jump across a discontinuity line
ε_1, ε_2, ε_3 major, intermediate, and minor principal strain respectively
ε_a axial strain in triaxial test
ε_q deviatoric strain (=2/3 ($\varepsilon_1 - \varepsilon_3$) in triaxial test)
ε_r, ε_z, ε_θ radial, vertical, and circumferential strain respectively
ε_{rev} reference strain corresponding to the point of last reversal in the Strain Dependent Modified Cam Clay Soil Model

Cam Clay model

ε_s engineering shear strain ($= \varepsilon_1 - \varepsilon_3$)
$\dot{\varepsilon}_1$ the largest principal strain increment
κ slope of unload-reload line in v-ln p' space
λ slope of one-dimensional compression line in v-ln p' space
v Poisson's ratio
σ bearing pressure of footing
ϕ angle of critical state friction

REFERENCES

Atkinson, J. H., Richardson, D. & Stallebrass, S. E. (1990). Effect of recent stress history on the stiffness of overconsolidated soil. *Géotechnique* **40**, No. 4, 531–540.

Bolton, M. D. & Powrie, W. (1988). Behaviour of diaphragm walls in clay prior to collapse. *Géotechnique* **38**, No. 2, 167–189.

Bolton, M. D. & Sun, H. W. (1991). Modelling of bridge abutments on stiff clay. *Proc. 10th Eur. Conf. Soil Mech., Florence* **1**, 51–55.

Bolton, M. D., Dasari, G. R. & Britto, A. M. (1994). Putting small strain non-linearity into Modified Cam Clay model. *Proc. 8th Conf. Int. Assoc. Computer Methods and Advances in Geomechanics*, *Morgantown, WV*, 537–542.

Brinch Hansen, J. (1970). A revised and extended formula for bearing capacity. *Dan. Geotech. Inst. Bull.* **28**, 5–11.

Burland, J. B. (1989). 'Small is beautiful': the stiffness of soils at small strains. 9th Laurits Bjerrum Memorial Lecture. *Can. Geotech. J.* **26**, No. 4, 449–516.

Butterfield, R. & Harkness, R. M. (1971). The kinematics of Mohr–Coulomb materials: stress–strain behaviour of soils. *Proceedings of the Roscoe Memorial Symposium*, Cambridge, pp. 220–233.

Chen, W. F. (1975). *Limit analysis and soil plasticity.* Amsterdam: Elsevier.

Cox, A. D. (1962). Axially symmetric plastic deformations in soils. II: Indentation of ponderable soils. *Int. J. Mech. Sci.* **4**, 371–380.

Cox, A. D., Eason, G. & Hopkins, H. G. (1961). Axially symmetric plastic deformations in soils. *Phil. Trans. R. Soc. London Ser. A* **254**, No. 1036, 1–45.

Dasari, G. R. (1996). *Modelling the variation of soil stiffness during sequential construction*. PhD dissertation, University of Cambridge.

Dasari, G. R. & Britto, A. M. (1995). *Strain-Dependent Modified*

Cam Clay model. Technical Report CUED-SOILS/TR276. Cambridge University Engineering Department, Cambridge.

Décourt, L. (1992). SPT in non classical material. *Proceedings of US-Brazil Geotechnical Workshop on Applicability of Classical Soil Mechanics Principles in Structured Soil, Belo Horizonte*, pp. 67–100.

Eason, G. & Shield, R. T. (1960). The plastic indentation of a semi-infinite solid by a perfectly rough circular punch. *J. Appl. Math. Phys. (ZAMP)* **11**, No. 1, 33–43.

Hibbit, Karlsson & Sorensen Inc. (2001). *ABAQUS/Standard user's manual, version 6·2*. Pawtucket, RI: Hibbit, Karlsson & Sorensen Inc.

Hight, D. W., Böese, R., Butcher, A. P., Clayton, C. R. I. & Smith, P. R. (1992). Disturbance of the Bothkennar clay prior to laboratory testing. *Géotechnique* **42**, No. 2, 199–217.

Hill, R. (1950). *The mathematical theory of plasticity*. Oxford: Clarendon Press.

Houlsby, G. T. & Wroth, C. P. (1991). Variation of shear modulus of a clay with pressure and overconsolidation ratio. *Soils Found.* **31**, No. 3, 138–143.

Houlsby, G. T. & Wroth, C. P. (1983). Calculation of stresses on shallow penetrometers and footings. *Proceedings of the IUTAM/IUGG symposium on seabed mechanics*, Newcastle upon Tyne, pp. 107–112.

Institution of Civil Engineers (1992). Bothkennar soft clay test site: characterization and lessons learned. *Géotechnique* **42**, No. 3, 161–378.

Jardine, R. J., Symes, M. J. & Burland, J. B. (1984). The measurement of soil stiffness in the triaxial apparatus. *Géotechnique* **34**, No. 3, 323–340.

Jardine, R. J., Potts, D. M., Fourie, A. B. & Burland, J. B. (1986). Studies of the influence of non-linear stress–strain characteristics in soil–structure interaction. *Géotechnique* **36**, No. 3, 377–396.

Jardine, R. J., Lehane, B. M., Smith, P. R. & Gileda, P. A. (1995). Vertical loading experiments on rigid pad foundations at Bothkennar. *Géotechnique* **45**, No. 4, 573–597.

Kusakabe, O., Suzuki, H. & Nakase, A. (1986). An upper bound calculation on bearing capacity of a circular footing on a non-homogeneous clay. *Soils Found.* **26**, No. 3, 143–148.

Lehane, B. M. (2003). Vertically loaded shallow foundation on soft clayey silt. *Proc. Inst. Civ. Engrs Geotech. Engng* **156**, No. 1, 17–26.

Levin, E. (1955). Indentation pressure of a smooth circular punch. *Q. Appl. Math.* **13**, No. 2, 133–137.

Masing, G. (1926). Eigenspannungen und Verfestigung beim Messing. *Proc. 2nd Int. Cong. Appl. Mech., Zurich*, 332–335.

Mayne, P. W. & Kulhawy, F. H. (1982). K_0–OCR relationship in soils. *ASCE J. Geotech. Engng* **108**, No. 6, 851–872.

Osman, A. S. (2005). *Predicting ground displacements in clay during construction*. PhD dissertation, Cambridge University.

Osman, A. S. & Bolton, M. D. (2004). A new design method for retaining walls in clay. *Can. Geotech. J.* **41**, No. 3, 451–466.

Shield, R. T. (1955a). On plastic flow of metal under conditions of axial symmetric bearing capacity of the clay. *Proc. R. Soc. London Ser. A*, **233**, No. 1193, 267–287.

Shield, R. T. (1955b). The plastic indentation of a layer by a flat punch. *Q. Appl. Math.* **13**, No. 1, 27–46.

Shield, R. T. & Drucker, D. C. (1953). The application of limit analysis to punch-indentation problems. *ASME J. Appl. Mech.* **20**, No. 4, 453–460.

Skempton, A. W. (1951). The bearing capacity of clay. *Proc. Building Res. Cong., London* **1**, 180–189.

Skempton, A. W. & Bjerrum, L. (1957). Contribution to the settlement analysis of foundations on clay. *Géotechnique* **7**, No. 4, 168–178.

Tani, K. & Craig, W. H. (1995). Bearing capacity of circular foundations on soft clay of strength increasing with depth. *Soils Found.* **35**, No. 4, 21–35.

Wood, D. M. (1990). *Soil behaviour and critical state soil mechanics*, 1st edn. Cambridge: Cambridge University Press.

Wroth, C. P. (1975). *In situ* measurement of initial stresses and deformation characteristics: state-of-the-art review. *Proceedings of the conference on in situ measurement of soil properties*, Raleigh, NC, Vol. 2, pp. 181–230.

Viggiani, G. & Atkinson, J. H. (1995). Stiffness of fine-grained soil at very small strains. *Géotechnique* **45**, No. 2, 249–265.

Yimsiri, S. (2002). Pre-failure deformation characteristics of soils: anisotropy and soil fabric. PhD thesis, Cambridge University.